



HAL
open science

Position Estimation using the Radical Axis Gauss Newton Algorithm: Experimental Analysis

Luis Arellano-Cruz, Giselle Galvan-Tejada, Rogelio Lozano

► **To cite this version:**

Luis Arellano-Cruz, Giselle Galvan-Tejada, Rogelio Lozano. Position Estimation using the Radical Axis Gauss Newton Algorithm: Experimental Analysis. *Journal of Intelligent and Robotic Systems*, 2023, 107 (1), 10.1007/s10846-022-01779-x . hal-04346802

HAL Id: hal-04346802

<https://hal.science/hal-04346802v1>

Submitted on 15 Dec 2023

HAL is a multi-disciplinary open access archive for the deposit and dissemination of scientific research documents, whether they are published or not. The documents may come from teaching and research institutions in France or abroad, or from public or private research centers.

L'archive ouverte pluridisciplinaire **HAL**, est destinée au dépôt et à la diffusion de documents scientifiques de niveau recherche, publiés ou non, émanant des établissements d'enseignement et de recherche français ou étrangers, des laboratoires publics ou privés.

Position Estimation using the Radical Axis Gauss Newton Algorithm: Experimental Analysis

Luis A. Arellano-Cruz
UMI LAFMIA Laboratory
Center for Research and Advanced Studies of
IPN
Mexico City, MEXICO.
e-mail: luis.arellano@cinvestav.mx

Giselle M. Galvan-Tejada
Communications Section, Department of
Electrical Engineering
Center for Research and Advanced Studies of
IPN
Mexico City, MEXICO.
e-mail: ggalvan@cinvestav.mx

Rogelio Lozano-Leal
CNRS UMR Heudiasyc-UTC,
Universites de Technologie de Compiègne
Compiègne, FRANCE.
e-mail: rogelio.lozano@hds.u

Abstract- Generally a UAV is mounted with multiple sensors to help in their navigation including altitude and position sensors. Although there are currently different sensors to determine the flight altitude, the acquisition of the position at every moment is a hard task to be achieved mainly in crowded scenarios where the multiple obstacles make difficult the transmission of signal coming from satellites (for global navigation systems) or base stations which do the functions of anchors in some localization systems. Another issue of this kind of scenarios is the low probability to obtain redundancy systems due to obstruction of the signal. For the case where there is only the minimum information required to estimate the position, in this work the RA-GN algorithm proposed before is applied to a localization system. In order to prove the achieved efficiency by the RA-GN algorithm as well as to analyze its accuracy, a measurement campaign was conducted in a semi-forest environment. Results reported here show that the RA-GN algorithm is able to improve the accuracy of estimation in real conditions into crowded environments, specially under critical situations where the signal is perturbed by the obstacles and even by the orientation of the tag respect to the anchors compared with other positioning methods.

I. Introduction

Nowadays, the positioning systems have been widely studied mainly for navigation applications of autonomous mobile robots (whether aerial, terrestrial or underwater). In order for these robots to move in the desired direction, it is essential to know their own position into the navigation scenario. In the literature there are different strategies addressed to solve the estimation problem which have been evaluated in diverse applications [1]. For example, the Wireless Sensor Networks (WSNs) are a natural testbed because their low cost of manufacturing, make them possible to deploy a great number of sensors into an interest area providing a high amount of information which is used to localize the sensors themselves [2].

The problem of localization for WSNs has been studied and solved by different approaches taking the physical properties of communication signals, e.g., Received Signal Strength Indicator (RSSI), Time of Arrival (ToA), Time Difference of Arrival (TDoA) and Angle of Arrival (AoA) [3]. In addition, ultra wideband (UWB) technology is commonly used for low range and indoor position estimation due to the high accuracy provided by the UWB signals characteristics [4],[5] and the low cost.

Currently, it is possible to find commercially UWB localization systems (e.g. DWM1000 modules [6]) which are able to estimate the position with an accuracy of 10 cm of error. However, this accuracy is achieved under ideal line of sight (LOS) conditions without obstacles that could affect the signal. Despite that restriction, Wu et al. [7] have demonstrated that combining UWB technology and the ToA parameter, it is possible to measure the distance between a transmitter and a receiver with an error of the order of 30-50 cm in crowded obstacles environments which could affect the estimation accuracy substantially.

On the other hand, most of the works found in the literature about localization for WSN are based on overdetermined systems, which benefit from the information provided by the redundancy of a great number of anchors since that is the easiest way to maximize the accuracy in the estimation [7-5]. However, there are situations where it is not possible to count with a greater number of anchors specially crowded obstacles scenarios where the signal is affected and attenuated by propagation phenomena such as shadowing and multipath fading. For these cases where it is only possible to connect with a minimum number of anchors, we proposed a new positioning algorithm called RA-GN algorithm [8] due to combine the Radical Axis (RA) concept and the well-known Gauss-Newton (GN) method to determine the position of an unmanned aerial vehicle (UAV) flying in outdoor scenarios with multiple obstacles. Considering that commonly a UAV can be equipped with different sensors (barometer, Light Detection and Ranging (LIDAR) or ultrasonic sensor) to determine the flight altitude, the problem of localization could be reduced to find the position in the XY plane which means that a minimum of three anchors are required.

In [8] the advantage of the RA-GN algorithm for the case where there is not redundancy in the localization system was presented and analyzed by simulation. In this work we show experimental results of the RA-GN algorithm [8] implemented in a testbed using a commercial UWB localization system and operating in a multipath environment where the signal is affected by the density of the obstacles. These experimental results are discussed based on an accuracy comparison between the RA-GN algorithm and the RA and GN methods used separately.

This work is organized as follows: Section II presents the proposed positioning method and the concepts of two positioning methods which are based on. In Section III the measurement campaign is described. In Section IV the results are presented and analyzed. Finally, the conclusions are discussed in Section V.

II. UWB positioning

Federal communications commission (FCC) define UWB as a signal transmission which bandwidth exceeds the lesser of 00 MHz. In 2002, the FCC opened the 3.1-10.6 and 22-29 GHz bands to UWB with a power spectral density limited within -41.33 dBm/MHz [9]. One of the UWB applications which has gain a great interest nowadays is the positioning systems. The use of UWB technology into Real Time Location Systems (RTLS) has shown the capability to obtain a high accuracy level with a magnitude of a few centimeters order, this is achieved due to the resolution provided by

nanosecond pulses [10]. In [11] five commercial RTLS with different competing technologies (UWB, Wi-Fi, ultrasonic, narrowband radio frequency (RF) and infrared (IR)) were tested and compared for tracking location purposes into a medical room. The UWB system demonstrated the best performance in terms of accuracy, however, also it has the most expensive cost and the lowest range.

Line-of-sight (LOS) conditions are necessary to provide the best accuracy possible into the measurements. However, in scenarios where a great number of obstacles are present the direct path propagation could be very often blocked and the conditions of Non-line-of-sight (NLOS) are most probable to find. Since the path propagation under NLOS conditions are longer than LOS conditions due to the reflections and diffraction of the signal by the obstacles, the ToA is uncertain which results in a greater error [12]. Another issue that affects the accuracy of the measured distances is the orientation-dependent error which could be a mix of different factors such as antenna design and its radiation diagram or the electronic circuit build around the antenna [13].

The most common solution for those problems is the use of redundancy which implies increase the number of anchors in order to provide a robust estimation [14]. In [15] the author showed that using different convolutional neural networks (CNNs) based on NLOS channel classification and ranging regression models combined with redundancy systems improve significantly indoor localization performance, in particular, the use of 10 anchors provides a mean localization error of 0.113 m for a WLS Location estimator with ranging error mitigation.

Nowadays there is a commercial UWB system widely used for industrial and research purposes due to the accuracy provided for indoor localization, the DWM1001 distributed by Decawave. However, in this work we decide test the Decawave Real-Time Localization Systems (DRTLS) in a semi-forest scenario which is an outdoor and crowded environment. In order to determine how the presence of trees affect the range of the UWB signal and the measurement distance between two modules we perform a series of measurements with different size of trees and compared with an open scenario free of obstacles. In Fig. 1 it can be observed a pair of DWM1001 modules A and B placed into two different scenarios with an altitude of 1.5 m, although both scenarios have LOS conditions, in the first scenario where there are not any obstacles that could affect the signal propagation the maximum range of d_{AB} obtained was about 18 m, after observe 500 samples we could observe that the measured distance have a mean error of 20.79 cm and a standard deviation of 10.19 cm, on the other hand, in the second studied scenario there are some trees around the modules which reduced the maximum range to 16 m but reducing the mean error to 3.03 cm and a standard deviation of 5.94 cm which make us suppose that multipath fading improves the accuracy for this specific case.



Fig. 1 Two different scenarios with LOS conditions: *a)* open scenario free of obstacles, *b)* semi-forest scenario with some trees around.

Similarly, we have the interest to observe how the measured distance between two DWM1001 modules are affected under NLOS conditions due to the obstruction by the trees, with that in mind the distances measured between modules was analyzed when trees of different size was placed into the trajectory between the modules. The Fig. 2 shows 4 different cases of NLOS conditions, the purpose of those test is observing the measured distance between the two modules when there is an object as obstruction.



1)



2)



3)



4)

Fig. 2 Four different scenarios with NLOS conditions: 1) a tall tree with a trunk of 35 cm of diameter, 2) a small tree with a trunk of 10 cm of diameter, 3) two trees with trunks of 25 and 30 cm of diameter, 4) a tall tree with a trunk of 35 cm of diameter and a small tree with 10 cm of diameter.

In the Table 1, the results of each case are shown in terms of the range and the values of the mean error and deviation standard.

Case	Range	Mean error	Deviation standard
1	4 m	3.02 cm	5.64 cm
2	10 m	10.05 cm	3.94 cm
3	4 m	2.59 cm	4.78 cm
4	3.5 m	7.7 cm	15.88 cm

Table 1 Measured distances with NLOS conditions.

It is possible to observe that range reached with NLOS conditions is too much smaller compared with the LOS conditions although the error obtained is low spatially for the cases 1 and 3 probably by the proximity. It is worth to mention that for a tall tree with 1 m of diameter between the

DWM1001 modules it was not possible to obtain measurements because they were not able to connect each other. Those tests demonstrate the difficulty to achieve a connection in a semi-forest environment with a high-density level of trees reducing the probability to obtain a redundancy system although the error in measured distances is not a great problem at least for small distances.

III. Description of the Measurements scenario

In order to demonstrate the efficiency of the RA-GN algorithm under practical conditions, we install four anchors and one tag surrounded by trees in a semi-forest scenario as shown in Fig. 3. This scenario is made up by pine trees over 10 meters high, with a density of 9 trees into an area of interest with a size of 8×8 m which is in the Center for Research and Advanced Studies of IPN in Mexico City, Mexico as is illustrated in Fig. 4. The position and diameter of each pine tree is shown in the Table 2. Measurements were carried out during winter 2021-2022 with no windy and dry weather.



Fig. 3 Four anchors and one tag in a semi-forest scenario.

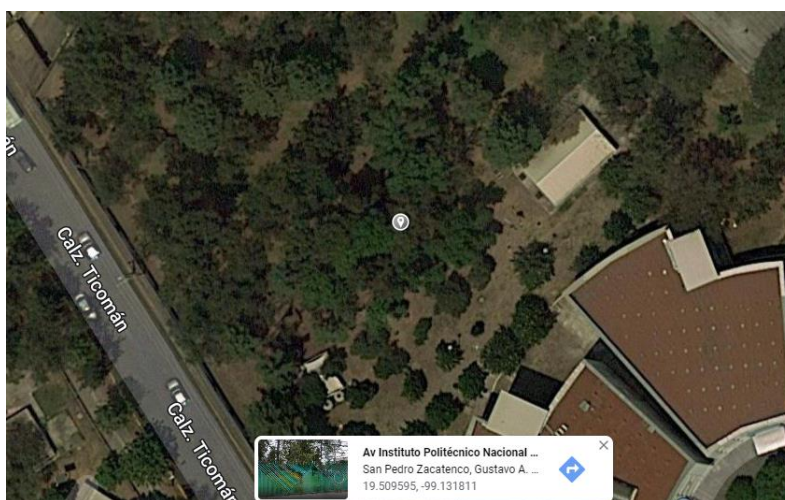


Fig. 4 Scenario view from google maps.

Position of the tree	Diameter of the tree
(1.4, -2)	40 cm
(1.2, -4.2)	35 cm
(-2.35, -1.4)	15 cm
(-2.35, -2.2)	40 cm
(5.1, 1.4)	30 cm
(5.1, 2.4)	35 cm
(-3.15, 2.68)	35 cm
(5.95, 5.85)	30 cm
(6.35, 1.75)	22 cm

Table 2 Position and diameter of each tree into the area of interest

The DMW1000 modules [6] which make use of the ToA parameter with UWB technology were used to measure the distance between the modules assigned as anchors and the module assigned as tag. In order to evaluate the RA-GN algorithm in this scenario, we move the tag module through the measurement field to avoid any perturbation introduced by dynamics of any UAV, but this module could be mounted in a UAV in a further experiment. The fixed positions of the anchors were $A_1(0,4)$, $A_2(-5,0)$, $A_3(5,0)$ and $A_4(0, -6)$ at 1.6 m of altitude while the tag module was located at 6 different positions over a tripod at the same altitude (1.6 m) in order to keep all modules aligned in a 2D plane. The positions analyzed are shown in the Table 3 along with the line-of-sight conditions for each anchor, it is possible to observe that there is at least one NLOS condition.

Positions	Line-of-sight conditions			
	A_1	A_2	A_3	A_4
(0, -3.7)	LOS	NLOS	LOS	LOS
(-4.6, 2.05)	LOS	LOS	LOS	NLOS
(7, 0)	NLOS	LOS	LOS	LOS
(3, -2.5)	LOS	NLOS	LOS	LOS
(-3.35, -4)	LOS	LOS	NLOS	LOS
(-4, -7)	NLOS	LOS	LOS	LOS

Table 3 Line-of-sight conditions of the tag respect each anchor.

The Fig. 5 display a diagram of the area of interest with the positions of the anchors, trees and the positions analyzed. Each position is estimated using the RA-GN algorithm and compared to the estimation provided by the DRTLS installed into the DWM1001 modules. Due to objective of this work is verify the accuracy of the RA-GN algorithm under different conditions, the orientation of the modules also will be considered into the tests. The anchors also will be in fixed orientation facing to the center of the area, where $\theta_1 = 270^\circ$, $\theta_2 = 0^\circ$, $\theta_3 = 180^\circ$ and $\theta_4 = 90^\circ$ for the respective anchors. On the other hand, then orientation of the tag θ is rotated each 20° from 0° to 340° at each position in order to observe how the orientation-dependent error affects the estimated position for both cases, the RA-GN algorithm and the DRTLS.

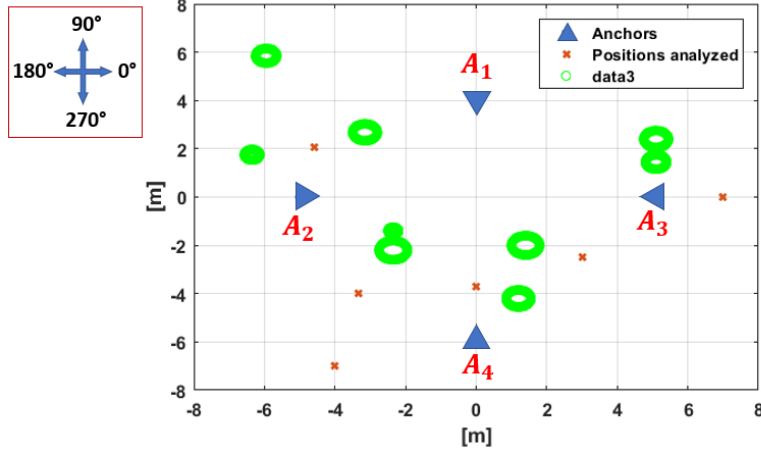


Fig. 5 Diagram of the experiment conducted.

IV. Results

The position of the tag is estimated by the RA-GN algorithm previously exposed. In order to compare the accuracy achieved with the estimation obtained by the DRTLS, we used as parameter of comparison the RMSE of the distance respect to the anchors used to estimate the position.

$$F(p) = \sqrt{\frac{1}{N} \sum_{i=1}^N e_i^2} \quad (1)$$

where N is the number of anchors used to estimate the position which could be 3 or 4 depending of the connection between the tag and the anchors. The error e_i will be calculated as the difference of the distances between the estimated position (\hat{x}, \hat{y}) and the anchor in the position (x_i, y_i) , compared with the measured distance \hat{d}_i between the tag and the anchor i .

$$e_i = \sqrt{(\hat{x} - x_i)^2 + (\hat{y} - y_i)^2} - \hat{d}_i$$

The results obtained were analyzed using the cumulative distribution function (CDF) of the RMSE with a total of 600 estimations for each position and each orientation where the tag was collocated. The Tables 4-15 show the information obtained by the tests conducted.

Firstly, in the Tables 4-9 we can compare the results obtained when it is considered only three anchors in the RA-GGN algorithm despising the information providing from the anchors with NLOS condition. The RMSE minimum obtained with a 90% of probability according to the CDF achieved by the RA-GN algorithm, $RMSE_{RAGN}$, is compared directly with the CDF of the RMSE obtained by the estimation provided by the DRTLS, $RMSE_{DRTLS}$. Also is displayed the percentage ρ_3 when the tag achieved to connect with at least 3 of the anchors in order to determine its position and the percentage when it was not possible ρ_0 . Another important information to be analyzed was the mean error of the measured distance respect to the real distance, μ_3 , and the deviation standard σ_3 .

The Table 4 shows the measurements obtained when the tag is placed in the position (0, -3.7) and is rotated each 20°. Although in most of the measurements the connection between the tag and the anchors is excellent, we can observe that an orientation of 120° was the only case when there was not possible to connect with at least 3 anchors proving that there is orientations which affect the connection between the tag and the anchors critically. On the other hand, in all the cases the RA-GN algorithm has a lower RMSE than the DRTLS, with a minimum difference of 0.1 cm and a maximum of 12.7 cm.

Position: (0, -3.7)						
θ	$RMSE_{DRTLS}$ (cm)	$RMSE_{RAGN}$ (cm)	ρ_3 (%)	ρ_0 (%)	μ_3 (cm)	σ_3 (cm)
0	16.9	12.2	98.66	1.33	8.38	6.10
20	15.2	10.9	99.50	0.50	7.59	6.91
40	15.3	11.4	100	0	7.83	5.81
60	23.7	11	99.66	0.33	7.43	6.93
80	12.1	12	100	0	9.55	8.27
100	10.4	8.9	99.83	0.16	9.52	7.46
120	-	-	-	100	-	-
140	10	9.1	100	0	5.68	3.73
160	10.7	10.1	100	0	7.5	4.20
180	10.7	10.1	100	0	7.5	4.22
200	19.3	11.9	99.66	0.33	12.11	4.22
220	19.1	12.2	100	0	12.69	5.29
240	14.6	12	99.5	0.50	9.74	5.68
260	14.5	10.8	100	0	10.84	5.69
280	15.3	11.1	100	0	9.2	5.31
300	14.2	10.4	98	2	7.11	4.91
320	18.3	13	92.5	7.50	9.65	5.93
340	18.3	13.9	99.16	0.083	9.96	6.49

Table 4 Obtained measurement in the position (0, -3.7) using three anchors.

The Table 5 shows the measurements obtained when the tag is placed in the position (-4.6, 2.05). In this position we can observe a greater problem of connection from 140° to 260° specially with an orientation of 200°, due to ρ_3 for this range of orientation is lower than 90%, it cannot be possible to compare the RMSE for both methods. In this position it is possible observe an increase in the mean error of the measured distances μ_3 compared with the previous position which results in a higher RMSE for DRTLS, however, in contrast the RA-GN algorithm proved a better resolution obtaining a minimum RMSE of 3.1 cm and reducing the RMSE in 33.7 cm in the worst case for DRTLS.

Position: (-4.6, 2.05)						
θ	$RMSE_{DRTLS}$ (cm)	$RMSE_{RAGN}$ (cm)	ρ_3 (%)	ρ_0 (%)	μ_3 (cm)	σ_3 (cm)
0	29.3	5.6	97.83	2.17	21.63	9.78
20	36.6	6.8	95.33	4.67	21.44	12.07
40	35.4	6.6	95	5	20.18	10.87
60	26.7	5.9	98.17	1.83	16.01	11.40
80	28.9	6	100	0	14.30	11.75
100	12.1	3.1	99.83	0.17	19.07	10.79
120	40.6	6.9	91.83	8.17	14.29	12.55

140	-	-	74.83	25.17	14.64	11
160	-	-	74.83	25.66	19.05	8.97
180	-	-	86.83	13.17	17.95	5.24
200	-	-	-	100	-	-
220	-	-	68	32	21.94	7.29
240	-	-	46.67	53.33	21.23	7.04
260	-	-	38.83	61.17	22.04	6.45
280	14.4	10.8	99.83	0.17	24.45	5.96
300	14.1	9.1	100	0	26.98	4.71
320	20.8	7.8	100	0	26.41	7.58
340	18.3	6.8	100	0	26.94	6.48

Table 5 Obtained measurement in the position (-4.6, 2.05) using three anchors.

The Table 6 shows the measurements obtained when the tag is placed in the position (7, 0). In this position the problems of connection increased since there are three cases where the estimation was not possible. On the other hand, the RMSE given by DRTLS is just above 10 cm thanks to the measured distances is too lower, still the RA-GN algorithm improve the estimation.

Position: (7,0)						
θ	$RMSE_{DRTLS}$ (cm)	$RMSE_{RAGN}$ (cm)	ρ_3 (%)	ρ_0 (%)	μ_3 (cm)	σ_3 (cm)
0	15.9	8.2	97.5	2.5	8.88	6.72
20	13.6	10.4	98.67	1.33	10.42	7.80
40	-	-	30.67	69.33	16.24	6.93
60	-	-	-	100	-	-
80	-	-	88.67	11.33	27.36	39.85
100	16.5	5.6	92.5	7.5	5.35	3.24
120	13.3	4.7	99.33	0.67	4.46	3.62
140	15.2	4.6	93.17	6.83	5.14	4.02
160	13.3	3	99.83	0.17	6.27	3.31
180	13.4	4	100	0	8.18	4.10
200	14.5	3.6	100	0	7.53	4.93
220	-	-	-	100	-	-
240	10.8	3.2	98	2	7.10	4.52
260	10.4	3.7	99.67	0.33	9.05	6.04
280	10.8	2.9	100	0	7.50	4.99
300	-	-	-	100	-	-
320	14.4	4.5	99.83	0.17	5.04	5.01
340	17.5	3.4	100	0	9.24	5.68

Table 6 Obtained measurement in the position (7,0) using three anchors.

In the Table 7 which shows the measurements obtained when the tag is placed in the position (3, -2.5) we can observe that with an orientation of 200° the connection is lost and for the orientation of 40° and 340° the connection is affected enough to ρ_3 will be lower than 90%. If we compare the values of RMSE obtained, the gain obtained by the RA-GN algorithm is just by few centimeters in most of the cases except by the orientation of 160° where the RMSE achieved is 13.3 cm lower than the provide by DRTLS.

Position: (3, -2.5)

θ	$RMSE_{DRTLS}$ (cm)	$RMSE_{RAGN}$ (cm)	ρ_3 (%)	ρ_0 (%)	μ_3 (cm)	σ_3 (cm)
0	6.7	4.1	98.67	1.33	18.08	3.83
20	8	5.4	95.83	4.17	21.04	4.62
40	-	-	44	56	31.46	9.84
60	15.3	12.3	99.17	0.83	26.59	11.33
80	30.5	26.8	100	0	39.61	26.43
100	11.9	10.7	100	0	25.54	8.13
120	5.5	3.3	99.50	0.50	16.57	3.33
140	5.5	3	99.50	0.50	18.23	4.70
160	16.6	3.3	100	0	22.56	6.06
180	12.5	10.1	99.83	0.17	17.08	10.50
200	-	-	-	100	-	-
220	14.7	12.5	99.67	0.33	18.30	7.93
240	7.7	6.3	100	0	20.72	5.32
260	8.8	6.4	99.83	0.17	15.25	5.92
280	7.8	5.5	99.33	0.67	17.01	5.15
300	6.5	4.1	98.83	1.17	19.06	3.66
320	5.8	3	99	1	16.76	3.52
340	-	-	80.83	19.67	15.30	4.07

Table 7 Obtained measurement in the position (3, -2.5) using three anchors.

In the Table 8 we can see that in the position (-3.35, -4) the greatest values of ρ_0 is 47% for an orientation of 240° which means that the connection between the tag and the anchors was more stable respect to the other positions but the error into the measured distances is greater as we can observe in the values of μ_3 (a maximum value of 300.4 cm) and σ_3 (maximum value of 401.53 cm) resulting in a higher estimation error. Although for the first case of 0° the RMSE is above of 1 m for both methods, on the other hand, in the case of 260° despite of the high error in measure distances the DRTLS is able to estimate the position with a RMSE of 20.9 cm and the RA-GN algorithm a RMSE of 9.4 cm obtaining a gain of 11.5 cm.

Position: (-3.35, -4)						
θ	$RMSE_{DRTLS}$ (cm)	$RMSE_{RAGN}$ (cm)	ρ_3 (%)	ρ_0 (%)	μ_3 (cm)	σ_3 (cm)
0	182.8	112.9	99.83	0.17	107.34	144.67
20	19	6.1	99.67	0.33	9.53	5.62
40	18.7	6.3	99.83	0.17	11.73	4.67
60	21.3	5.7	99.83	0.17	9.32	4.18
80	17.5	5.4	100	0	4.95	2.87
100	16.4	5.5	100	0	3.41	2.32
120	7.6	5.8	100	0	6.71	6.01
140	18	6.9	92.5	7.50	7.79	7.07
160	7.9	3.6	99.67	0.33	4.20	2.68
180	-	-	87.5	12.5	40.02	166.78
200	-	-	87.5	10.85	12.34	6.60
220	5.6	8.2	96.5	3.5	11.70	6.23
240	-	-	53	47	31.29	108.97
260	20.9	9.4	99.5	0.50	300.46	401.53
280	11.9	3.8	100	0	21.91	10.65
300	19.4	7.4	100	0	26.32	15.25

320	19.9	8.1	99.67	0.33	15.80	3.86
340	14.9	11.8	100	0	13.18	6.53

Table 8 Obtained measurement in the position (-3.35, -4) using three anchors.

Finally, in the Table 4 it is possible to observe that the position (-4, -7) is a point with really difficult problems of connection due to the high distance and interference by the trees between the tag and the anchors A_1 and A_3 . The test demonstrated that only five cases achieved more than 90% of connection with at least three anchors which shows like the previous positions the RA-GN algorithm obtain a lower RMSE by a few centimeters.

Position: (-4, -7)						
θ	$RMSE_{DRTLs}$ (cm)	$RMSE_{RAGN}$ (cm)	ρ_3 (%)	ρ_0 (%)	μ_3 (cm)	σ_3 (cm)
0	14.3	11.4	99.83	0.17	8.42	4.72
20	-	-	84.83	15.17	8.40	7.33
40	14.3	10.9	98	2	8.03	5.10
60	-	-	91.17	8.83	8.51	4.28
80	-	-	86.5	13.5	6.91	6.91
100	-	-	-	100	-	-
120	13.2	8.3	99.67	0.33	9.23	7.83
140	9.8	7.1	99.67	0.33	9.34	6.53
160	-	-	89.83	10.17	39.03	54.78
180	-	-	-	100	-	-
200	-	-	9.67	90.33	9.38	7.22
220	-	-	22.17	77.83	17.77	59.17
240	-	-	12.67	87.33	16.63	10.81
260	-	-	55.17	44.87	8.73	5.34
280	-	-	19.83	80.17	24.77	19.17
300	-	-	88	12	17.19	10.14
320	-	-	19.5	20.5	11.26	7.39
340	14.9	9.9	100	0	8.01	07.81

Table 9 Obtained measurement in the position (-4, -7) using three anchors.

The previous results demonstrated the efficiency of the RA-GN algorithm for estimation of position with no redundancy systems, with only three anchors. However, since there was a total of four anchors deployed in the area of interest some of the estimations given by the DRTLs were calculated with the information of the four anchors, the percentage ρ_4 represents the time when the tag count with the information of the four anchors during the measurements. In the Tables 10-15 are shown the specific cases where DRTLs gives an estimation with four anchors and is compared with the estimation calculated by the RA-GN algorithm adding the anchors with NLOS conditions.

The Table 10 shows the measurements obtained in the position (0, -3.7) adding the mean error μ_{NLOS} and the standard deviation σ_{NLOS} of the NLOS measured distance which for the orientations of 40°, 60° and 300° are very high, then, when the measured distances of the four anchors are considered the value of the mean error μ_4 and standard deviation σ_4 increase considerably. In this case the information coming from the anchor with NLOS conditions affect the accuracy of the estimation obtained by the RA-GN algorithm, in general the RMSE increase compared with the estimation calculated with only three anchors mainly for the orientations 40° and 60°, where the

RMSE obtained by the RA-GN is higher to the obtained by DRTLs. In the case of 300% the percentage of ρ_4 is very low to affect the RMSE.

Position: (0, -3.7)							
θ	$RMSE_{DRTLs}$ (cm)	$RMSE_{RAGN}$ (cm)	ρ_4 (%)	μ_{NLOS} (cm)	σ_{NLOS} (cm)	μ_4 (cm)	σ_4 (cm)
40	15.3	89.9	92	258.12	160.66	66.57	93.41
60	23.7	35.6	88.83	114.13	106.83	31.83	55.74
80	12.1	11.9	99.16	4.91	22.15	8.40	13.20
100	10.4	9.3	81	5.23	22.88	8.62	12.48
140	10	8.9	100	5.65	23.76	5.67	12.16
160	10.7	10	100	6.89	25.13	7.35	13.38
180	10.7	10	94.83	6.13	26.25	7.05	13.23
200	19.3	13.1	92.66	4.79	21.89	10.39	11.36
220	19.1	12.6	94.50	4.95	22.24	10.83	11.93
240	14.6	11.7	77.66	5.54	23.54	8.89	11.85
260	14.5	10.4	25.16	6.71	25.91	10.52	9.05
300	14.2	9.1	2	130.50	114.24	7.98	10.57

Table 10 Obtained measurement in the position (0, -3.7) using four anchors.

In the Table 11-15 we can observe that in most of the cases the Information provided by the anchor with NLOS condition do not have a μ_{NLOS} very high even it is not different of the other three anchors, thus, the RMSE obtained by the RA-GN is not affected too much compared with the obtained by the estimation given by only three anchors. There are cases like the Table 14 with an orientation of 0° where μ_{NLOS} is too lower than the μ_4 , the reason is that the anchor with more error is not the NLOS conditions but the furthest.

Position: (-4.6, 2.05)							
θ	$RMSE_{DRTLs}$ (cm)	$RMSE_{RAGN}$ (cm)	ρ_4 (%)	μ_{NLOS} (cm)	σ_{NLOS} (cm)	μ_4 (cm)	σ_4 (cm)
60	26.7	8.2	24.16	15.15	38.92	16.04	15.32
80	28.9	7.1	98.50	14.48	38.05	14.34	21.49
100	12.1	8.7	98.16	13.87	37.25	17.80	20.77
120	40.6	6.8	1.66	11.52	33.95	14.69	12.95
280	14.4	11.1	98.5	13.31	36.49	21.71	19.02
300	14.1	9.6	99.5	15.38	39.21	24.09	20.15
320	20.8	8	99.33	18.87	43.44	24.53	22.70
340	18.3	7.2	98.5	18.73	43.28	24.91	22.31

Table 11 Obtained measurement in the position (-4.6, 2.05) using four anchors.

Position: (7, 0)							
θ	$RMSE_{DRTLs}$ (cm)	$RMSE_{RAGN}$ (cm)	ρ_4 (%)	μ_{NLOS} (cm)	σ_{NLOS} (cm)	μ_4 (cm)	σ_4 (cm)
0	15.9	8.2	39.5	4.83	21.97	8.47	9.85
80	-	-	6.33	5.46	23.36	26.89	39.56
120	13.3	4.7	96.66	5.37	23.17	4.68	11.85
140	15.2	4.6	90.33	2.97	17.22	5.42	12.66
160	13.3	3	99.83	8	28.29	6.76	14.62

180	13.4	4.7	99.67	9.51	30.84	7.47	15.86
200	14.5	4.4	99.67	12.01	34.65	7.86	17.80
240	10.8	3.8	84.83	3.70	19.23	6.35	9.91
260	10.4	4.2	99	6.31	25.12	8.37	13.58
280	10.8	3.6	99.83	5.12	22.62	6.90	12.11
320	14.4	5.3	99.17	4.46	21.11	4.90	11.38
340	17.5	4.8	98.17	3.85	19.63	7.91	10.98

Table 12 Obtained measurement in the position (7, 0) using four anchors.

Position: (3, -2.5)							
θ	$RMSE_{DRTLS}$ (cm)	$RMSE_{RAGN}$ (cm)	ρ_4 (%)	μ_{NLOS} (cm)	σ_{NLOS} (cm)	μ_4 (cm)	σ_4 (cm)
60	15.3	12.3	3	24.47	49.47	26.40	11.60
80	30.5	26.8	98.67	22.86	47.81	35.54	33.34
100	11.9	10.7	97.83	25.22	50.22	20.56	14.09
120	5.5	3.3	21.17	17.90	42.30	21.05	24.24
160	16.6	3.3	72.33	29.83	54.61	26.18	29
220	14.7	12.5	2.33	27.62	52.56	27.31	32.53
240	7.7	6.3	54.67	21.43	46.29	23.57	25.20

Table 13 Obtained measurement in the position (3, -2.5) using four anchors.

Position: (-3.35, -4)							
θ	$RMSE_{DRTLS}$ (cm)	$RMSE_{RAGN}$ (cm)	ρ_4 (%)	μ_{NLOS} (cm)	σ_{NLOS} (cm)	μ_4 (cm)	σ_4 (cm)
0	182.8	132.6	99.5	7.13	26.70	84.61	126.31
20	19	12.1	98.83	8.74	29.57	8.93	15.62
40	18.7	12.1	83.5	14.19	37.67	9.81	18.20
60	21.3	10.8	99	11.23	33.51	8.34	17.13
80	17.5	10.5	99.83	3.87	19.67	7.14	10.85
100	16.4	6.8	90.33	2.93	17.11	6.48	10.15
180	-	-	3.67	4.42	21.03	39.58	165.78
280	11.9	11.9	86.67	28.03	52.94	23.28	26.79
300	19.4	15.2	99.67	3.10	17.61	20.53	16.64
320	19.9	11.2	99.33	2.83	16.83	12.57	9.46
340	14.9	13.1	99.33	2.58	16.07	10.54	10.08

Table 14 Obtained measurement in the position (-3.35, -4) using four anchors.

Position: (-4, -7)							
θ	$RMSE_{DRTLS}$ (cm)	$RMSE_{RAGN}$ (cm)	ρ_4 (%)	μ_{NLOS} (cm)	σ_{NLOS} (cm)	μ_4 (cm)	σ_4 (cm)
0	14.3	11.4	99.67	6.33	25.16	7.90	13.22
40	14.3	10.9	97.5	5.28	22.98	7.35	12.25
60	-	-	89.83	8.83	22.90	7.74	11.74
80	-	-	86	13.5	21.25	6.35	11.10
120	13.2	8.3	99.3	4.34	20.83	8.01	12.45
140	9.8	7.1	98.83	6.81	26.09	8.71	14.18
320	-	-	54.83	8.05	23.38	10.73	13.32
340	14.9	9.9	99.67	10.51	32.42	8.64	17.56

Table 9 Obtained measurement in the position (-4, -7) using four anchors.

With this, we have demonstrated the improvement in accuracy obtained by the RA-GN algorithm compared with one of the localization systems which is commercially available in the market under practical conditions. Although in most of the results obtained the gain of accuracy is only by few of centimeters, there is critical situations which could be a combination of some factors, such as the orientation of the tag, the perturbation added by the trees and the lack of information for the use of no redundant systems, but in those critical situations the RA-GN results to reduce the RMSE in order from 10 to 30 cm which is great gain for the purposes of positioning.

V. Conclusions

This work presents an evaluation of the RA-GN algorithm implemented in a practical scenario. The accuracy achieved with this algorithm for non-redundant systems is demonstrated using real measurements into a semi-forest scenario and compared in terms of accuracy with the estimation obtained by a commercial localization system. The results obtained after the measurement campaign demonstrate the improvement presented by the RA-GN algorithm. This strategy results to be an excellent option for autonomous robot navigation, especially for UAV which have the possibility to obtain the altitude by other sensors reducing the problem of positioning to the plane XY . In scenarios when the signal communication between anchors and UAV is disturbed by obstacles, it is impossible to count with redundancy improving the accuracy in the localization and the orientation of the UAV respect to the anchors results in the lack of antenna gain, the RA-GN algorithm results to be the best option to estimate the position increasing the accuracy. Thus, it is possible to navigate with greater precision in scenarios where the probability to suffer collision is high.

Acknowledgment

Authors want to thank the support given by Consejo Nacional de Ciencia y Tecnología (CONACYT), Mexico, through a postgraduate scholarship and the project 314879 "Laboratorio Nacional en Vehículos Autónomos y Exoesqueletos LANAVEX".

Bibliography

- [1] A. Yassin *et al.*, "Recent Advances in Indoor Localization: A Survey on Theoretical Approaches and Applications," in *IEEE Communications Surveys & Tutorials*, vol. 19, no. 2, pp. 1327-1346, Secondquarter 2017, doi: 10.1109/COMST.2016.2632427.
- [2] T. J. Black, P. N. Pathirana and S. Nahavandi, "Position estimation and tracking of an autonomous mobile sensor using received signal strength," *2008 International Conference on Intelligent Sensors, Sensor Networks and Information Processing*, 2008, pp. 19-24, doi:10.1109/ISSNIP.2008.4761956.

- [3] V. K. Chaurasiya, N. Jain and G. C. Nandi, "A novel distance estimation approach for 3D localization in wireless sensor network using multidimensional scaling," *Inf. Fusion*, vol 15, pp 5–18, January 2014. doi:10.1016/j.inffus.2013.06.003.
- [4] S. Gezici and H. V. Poor, "Position Estimation via Ultra-Wide-Band Signals," in *Proceedings of the IEEE*, vol. 97, no. 2, pp. 386-403, Feb. 2009, doi:10.1109/JPROC.2008.2008840.
- [5] A. Poulouse, Ž. Emeršič, O. Steven Eyobu, D. Seog Han, "An accurate indoor user position estimator for multiple anchor UWB localization," *2020 International Conference on Information and Communication Technology Convergence (ICTC)*, Jeju Island, Korea (South), pp 478-482, 2020. doi:10.1109/ICTC49870.2020.9289338.
- [6] <https://www.decawave.com/product/dwm1000-module/>
- [7] S. Wu, Y. Ma, Q. Zhang and N. Zhang, "NLOS error mitigation for UWB ranging in dense multipath environments," *2007 IEEE Wireless Communications and Networking Conference*, Hong Kong, China, pp. 1565-1570, 2007. doi:10.1109/WCNC.2007.295.
- [7-5] I. Oppermann, M. Hämäläinen, J. Linatti, "UWB: theory and applications", John Wiley & Sons, 2004.
- [8] L. A. Arellano-Cruz, G. M. Galvan-Tejada and R. Lozano-Leal, "A New Positioning Algorithm Robust to Measured Distances Errors for Non-Overdetermined Systems," *2021 18th International Conference on Electrical Engineering, Computing Science and Automatic Control (CCE)*, 2021, pp. 1-4, doi:10.1109/CCE53527.2021.9633061.
- [9] FCC, First. "Report and order, revision of part 15 of the commission's rules regarding ultra-wideband transmission systems." *FCC02-48, April* (2002).
- [10] Cazzorla, Alessandro, et al. "A 5.6-GHz UWB position measurement system." *IEEE Transactions on Instrumentation and Measurement* 62.3 (2012): 675-683.
- [11] D. Clarke and A. Park, "Active-RFID System Accuracy and Its Implications for Clinical Applications," *19th IEEE Symposium on Computer-Based Medical Systems (CBMS'06)*, 2006, pp. 21-26, doi: 10.1109/CBMS.2006.33.
- [12] WU, Huiming; YANG, Jiankang; CHANG, Cheng. A Regional Positioning Algorithm for Non-line-of-sight (NOLS) Propagation. En *2019 International Conference on Computer, Network, Communication and Information Systems (CNCI 2019)*. Atlantis Press, 2019. p. 217-221.
- [13] KRAPEŽ, Peter; VIDMAR, Matjaž; MUNIH, Marko. Distance measurements in UWB-radio localization systems corrected with a feedforward neural network model. *Sensors*, 2021, vol. 21, no 7, p. 2294.
- [14] JIMÉNEZ, Antonio R.; SECO, Fernando. Improving the Accuracy of Decawave's UWB MDEK1001 Location System by Gaining Access to Multiple Ranges. *Sensors*, 2021, vol. 21, no 5, p. 1787.
- [15] Bregar, K.; Mohorčič, M. Improving Indoor Localization Using Convolutional Neural Networks on Computationally Restricted Devices. *IEEE Access* 2018, 6, 17429–17441.